Delayed S-cone sensitivity losses following the onset of intense yellow backgrounds linked to the lifetime of a photobleaching product?

Andrew Stockman

UCL Institute of Ophthalmology,
University College London, London, UK ✉

G. Bruce Henning

UCL Institute of Ophthalmology,
University College London, London, UK

Hannah E. Smithson

Department of Experimental Psychology,
University of Oxford, Oxford, UK

Andrew T. Rider

UCL Institute of Ophthalmology,
University College London, London, UK

Thirty years ago, Mollon, Stockman, & Polden (1987) reported that after the onset of intense yellow 581-nm backgrounds, S-cone threshold rose unexpectedly for several seconds before recovering to the light-adapted steady-state value—an effect they called: "transient-tritanopia of the second kind" (TT2). Given that 581-nm lights have little direct effect on S-cones, TT2 must arise indirectly from the backgrounds' effects on the L- and M-cones. We attribute the phenomenon to the action of an unknown L- and M-cone photobleaching product, X, which acts at their outputs like an "equivalent" background light that then inhibits S-cones at a cone-opponent, second-site. The time-course of TT2 is similar in form to the lifetime of X in a two-stage, first-order biochemical reaction A→X→C with successive best-fitting time-constants of 3.09 ± 0.35 and 7.73 ± 0.70 s. Alternatively, with an additional slowly recovering exponential "restoring-force" with a best-fitting time-constant 23.94 ± 1.42 s, the two-stage best-fitting time-constants become 4.15 ± 0.62 and 6.79 ± 1.00 s. Because the time-constants are roughly independent of the background illumination, and thus the rate of photoisomerization, A→X is likely to be a reaction subsidiary to the retinoid cycle, perhaps acting as a buffer when the bleaching rate is too high. X seems to be logarithmically related to S-cone threshold, which may result from the logarithmic cone-opponent, second-site response compression after multiplicative first-site adaptation. The restoring-force may be the same cone-opponent force that sets the rate of S-cone recovery following the unusual threshold increase following the *offset* **of dimmer yellow backgrounds, an effect known as "transient-tritanopia" (TT1).**

Introduction

Human photopic vision begins with the absorption of photons by the three classes of cone photoreceptor: the long- (L-), middle- (M-), and short- (S-) wavelength sensitive cones, which peak in sensitivity near 566, 541, and 441 nm, respectively (Stockman & Sharpe, 2000) to produce a trichromatic representation of the visual image. The outputs of the three cones then feed into several postreceptoral pathways that selectively encode different aspects of the image, such as color and brightness.

In this paper, we revisit an extensive and time-consuming series of measurements made in 1987 that characterized an intriguing visual phenomenon called "transient tritanopia of the second kind" (TT2) (Mollon, Stockman, & Polden, 1987). TT2 refers to the substantial and delayed loss of S-cone mediated sensitivity that follows the onset of intense yellow background lights, even though the yellow lights have relatively little direct effect on the S-cones (Mollon, 1982b; Mollon et al., 1987). This phenomenon is one of several "anomalies" of S-cone mediated vision (Mollon & Polden, 1977; Stiles, 1978; Pugh & Mollon, 1979; Polden & Mollon, 1980; Mollon, 1982a) attributed in

Received March 15, 2018; published June 21, 2018

Copyright 2018 The Authors

part to the restriction of S-cone signals within cone-opponent pathways, because there appears to be no *direct* S-cone input to the luminance pathway (e.g., Schrödinger, 1925; Luther, 1927; Walls, 1955; de Lange, 1958b; Guth, Alexander, Chumbly, Gillman, & Patterson, 1968; Smith & Pokorny, 1975; Boynton, 1979; Eisner & MacLeod, 1980; Lee & Stromeyer, 1989; Stockman, MacLeod, & DePriest, 1991; Ripamonti, Woo, Crowther, & Stockman, 2009).

The purpose of the current work was to develop a model to account for the delayed S-cone suppression and to relate the suppression to possible underlying biochemical and neural substrates. We start by considering how signals from the L- and M-cones could reduce S-cone sensitivity. The upper panel of Figure 1 shows a cone-opponent model of the main S-cone visual pathway proposed by Pugh and Mollon (1979) to account for the properties of S-cone mediated vision. Signals from the L-, M-, and S-cones, represented by colored triangles on the left of the panel, feed into a cone-opponent neural circuit that differences S-cone signals from the sum of the L- and M-cone signals. The sensitivity of the pathway is modulated at two sites: (a) at the cone photoreceptors, known as "first-site" adaptation and indicated by the circular feedback arrows on the cones, and (b) at a postreceptoral site after the cones, known as "second-site" adaptation (see, for example, Stockman & Brainard, 2010). In Figure 1, second-site "adaptation" is produced by a sigmoidal nonlinearity (as in figure 6 of Polden & Mollon, 1980) that can compress the neural response and thus reduce sensitivity to change. The second-site nonlinearity in Figure 1 is represented by the graph showing the response to the cone-opponent input with S-cone input increasing to the right and L+M cone input increasing to the left. Sensitivity at the output will be reduced if the input is shifted from the operating point (set by adaptation to a relatively long-lasting steady state input) either in the S-cone direction (by a violet-appearing light that preferentially excites the S-cones) or in the L+M cone direction (by, say, a yellow-appearing light that preferentially excites the L- and M-cones). This type of sensitivity regulation is known as response compression. As illustrated, the production of a criterion threshold response (ΔR) requires a much bigger change in the S-cone input (ΔS_1) when the input shifted towards either extreme than when L+M and S inputs are more balanced (ΔS_2). It is the effect on increment detection when the L+M signal predominates that concerns us in these experiments. Note that there is also a "restoring force" shown by the red arrow that acts to reduce any persistent polarization towards either L+M or S, which we will discuss next. (The particular way in which the second-site adaption is implemented is not critical in this context.)

Postreceptoral neural interaction
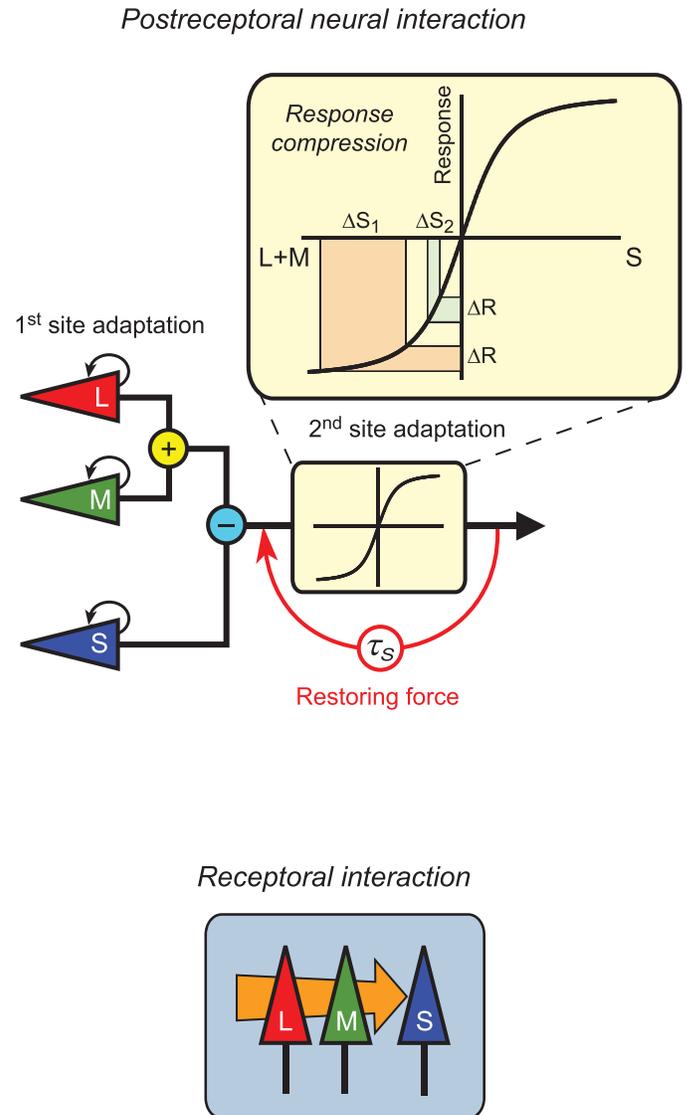

Receptoral interaction

Figure 1. Upper: Version of the Pugh and Mollon (1979) model in which the cone-opponent, second-site desensitization is implemented by a static nonlinearity (Polden & Mollon, 1980). The nonlinearity is a sigmoidal function that compresses the response at large inputs either in the +S or −(L+M) direction or in the L+M or (−S) direction. The effect of the nonlinearity can be understood by assuming that the system needs a fixed change in response (ΔR) in order for a change in the input to be detected. With small excursions near the center of the graph, ΔS_2, a smaller change is required to produce the criterion response, ΔR, than for the change in signal, ΔS_1, required at either extreme. Sensitivity should be greatest when the input is balanced, and the operating point of the system is in the middle of the response range. A restoring force acts with an exponential time constant of τ_S to reduce the polarization at the second-site (red arrow). Lower: Model in which the orange arrow from the L- and M-cones to the S-cones indicates a suppressive interaction that might arise because of a substance that permeates between cones, or because of competition for limited resources.

A consequence of the restriction of S-cone signals mainly to cone-opponent pathways, such as the one modelled in Figure 1, is that S-cone sensitivity measured psychophysically will be modulated by lights that excite the L- and M-cones as well as by lights that modulate the S-cones.

The delayed loss of S-cone sensitivity following the onset of an intense yellow background was named transient tritanopia of the second kind (TT2) to differentiate it from transient tritanopia (of the first kind or TT1), which refers to the S-cone sensitivity loss following the *offset* of long-wavelength adapting backgrounds of less than about 5 $\log_{10}$ Td (Stiles, 1949; Mollon & Polden, 1975; Mollon & Polden, 1976; Augenstein & Pugh, 1977; Mollon & Polden, 1977). The restoring force shown in Figure 1 with a time constant of τ_S was a force postulated by Pugh and Mollon (1979) to account for the roughly exponential recovery of $\log_{10}$ S-cone sensitivity in TT1 following the offset of the long-wavelength background. Probably the best psychophysical measurements of the time course of recovery of TT1 are those by Augenstein and Pugh (1977), who in a series of measurements on two observers found mean time constants ± 1 *SE* of 15.45 $\pm$ 1.05 and 27.57 $\pm$ 3.28 s (see their table 1). These time constants may be relevant to our second model, below. The lower illustration in Figure 1 will be described later.

The TT2 phenomenon can be seen in Figures 2 and 3, in which we have replotted data from figures 2 through 6 of Mollon, Stockman, and Polden (1987). Both figures show the logarithm of the thresholds for detecting a 1.54° diameter, 200-ms duration, 436-nm target flash (plotted as $\log_{10}$ quanta s^{-1} deg^{-2}) as a function of the time after the onset of various 6.5° diameter, 581-nm backgrounds. The background retinal illuminances, which are indicated by the different symbols shown in the key, ranged from 3.45 to 5.58 $\log_{10}$ photopic trolands (Td). For clarity, the data in both figures, which have been reproduced to facilitate comparisons between the different models, have been vertically shifted in successive steps of 0.5 $\log_{10}$ unit relative to the data shown by the green diamonds, which are plotted correctly with respect to the ordinate. The unshifted data can be seen in the original publication.

The TT2 phenomenon can be seen clearly after the onset of 581-nm backgrounds of 4.75 $\log_{10}$ Td and brighter, after which S-cone threshold rises to reach a peak after about 5 s, and then falls monotonically towards a steady-state value. By contrast, after the onset of backgrounds of lower illuminances, the peak sensitivity loss, which is typically less than about 0.5 $\log_{10}$ unit, coincides with the onset of the adapting field and recovers monotonically over time. This latter pattern is more similar to classical data obtained with achromatic flashes and backgrounds of comparably low illuminances of 3.70 $\log_{10}$ Td or less (Baker, 1949).

In order to follow the rapid changes in sensitivity, Mollon, Stockman, and Polden (1987) adopted a time-consuming method that they named the "Method of a Thousand Staircases," which was originally devised by Cornsweet and Teller (1965). Full methodological details for the TT2 measurements, which extended over 120 s, can be found in the original paper (Mollon et al., 1987). Given that we are mainly interested in the initial rise and fall in S-cone threshold, we show only the first 60 s after background onset.

The intense 581-nm backgrounds that produce the TT2 phenomenon strongly excite the L- and M-cones, but have relatively little direct effect on S-cones, which are over 4 $\log_{10}$ units less sensitive to the background light of 581 nm than to the 436-nm targets to be detected (Stockman, Sharpe, & Fach, 1999). Consequently, TT2 must depend primarily upon on an interaction between the L- and M-cones and the S-cones (Mollon et al., 1987). Additionally, given the cone spectral sensitivity differences between the 436-nm target and 581-nm background wavelengths, the detection of the 436-nm targets in these experiments should be *mediated* predominantly by S-cones, although S-cone sensitivity will be *modulated* by the L- and M-cones by way of second-site interactions. We can estimate the relative cone sensitivities to these lights from standard cone spectral sensitivity functions (Stockman & Sharpe, 2000). At 581 nm the S-cone quantal spectral sensitivity has fallen by 4.12 $\log_{10}$ units below its peak sensitivity at 440 nm. By contrast, the L- and M-cone quantal sensitivities have fallen by only 0.02 and 0.23 $\log_{10}$ unit, respectively, below their peaks; whereas at 436-nm, the L-, M-, and S-cone quantal spectral sensitivities have fallen 1.34, 1.17, and 0.03 $\log_{10}$ units, respectively, below their peaks. Thus, the brightest 581-nm background used in these experiments of 5.58 $\log_{10}$ trolands, which is 11.76 $\log_{10}$ quanta s^{-1} deg^{-2} is (after factoring in the relative insensitivity of the S cones to this wavelength) equivalent to a background of 7.64 $\log_{10}$ quanta s^{-1} deg^{-2} for the S-cones at 436 nm. This is only slightly above the dimmest detectible 436 nm target flash in this condition and cannot possibly account for the large initial rise and fall in threshold after background onset.

Our aim is to provide a simple, qualitative, descriptive model that can plausibly account for how signals from the L- and M-cones cause the delayed suppression of S-cone sensitivity seen in Figures 2 and 3. We consider the TT2 phenomenon to be especially important because it allows us to measure the effects of extreme light adaptation and bleaching in the L- and M-cones by their indirect effects on the S-cones.

Next, we consider the likely origin of the delayed suppression generated by the L- and M-cones.

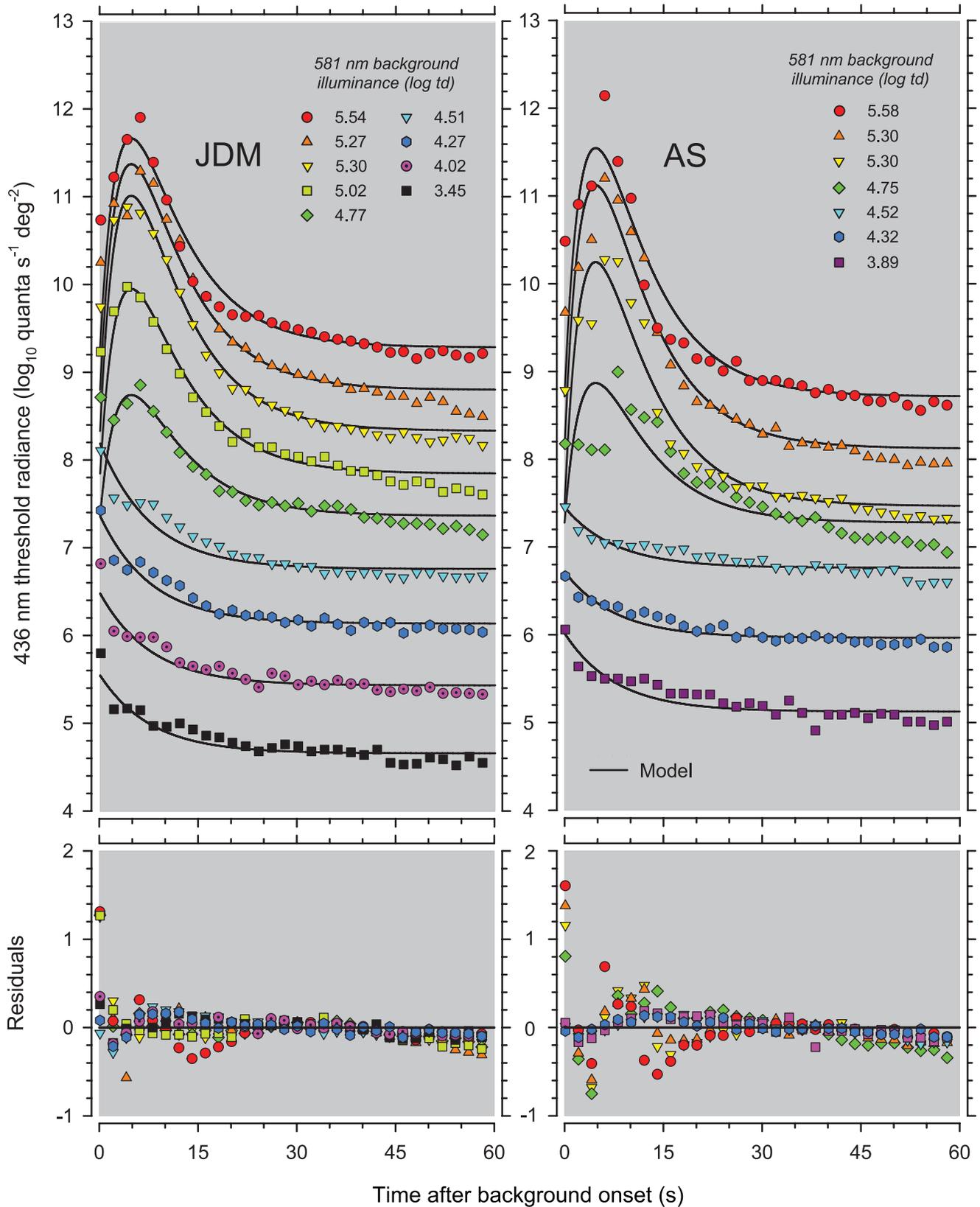Figure 2. Upper: Threshold radiances ($\log_{10}$ quanta s^{-1} deg^{-2}) for JDM (left panel) and AS (right panel) required to detect 200-ms, 436-nm target flashes as a function of time (seconds, linear scale) after the onset of 581-nm backgrounds of different retinal illuminances. The background illuminances for JDM were 5.54 (red circles), 5.27 (orange triangles), 5.30 (yellow inverted triangles),

→

←

5.02 (lime-green squares), 4.77 (green diamonds), 4.51 (cyan inverted triangles), 4.27 (blue hexagons), 4.02 (dotted violet circles), and 3.45 (black squares) $\log_{10}$ phot Td, whereas those for AS were 5.58 (red circles), 5.30 (orange triangles), 5.30 (yellow inverted triangles), 4.75 (green diamonds), 4.52 (cyan inverted triangles), 4.32 (blue hexagons), and 3.89 (violet squares) $\log_{10}$ phot Td. The data for JDM are from figure 3 of Mollon, Stockman, and Polden (1987), except for the data denoted by the inverted yellow triangles, which are from their figure 5. The data for AS are from their figure 4, except for the data denoted by the red circles, which are from their figure 2 and those denoted by the inverted yellow triangles, which are from their figure 6. The data shown by the green diamonds are plotted correctly with respect to the ordinate. The other data have been shifted up or down in successive 0.5 log unit steps for clarity. The solid lines show fits of the Basic model with two time-constants simultaneously fitted to all the data in both panels. For details, see Table A1 and text. Lower: Residuals ($\log_{10}$ threshold radiance) as a function of time (s). Symbols as in upper panel.

Basic model

Immediately after background onset, mechanisms of light adaptation will begin to reduce the sensitivities of the L- and M-cones. These mechanisms will include what have been called multiplicative adaptation—in which the overall gain of the system is reduced, subtractive adaptation—in which steady signals, such as those produced by the background, are discounted, and response compression—in which larger signals are compressed by nonlinearities in the photoreceptor or visual pathways (see, Barlow, 1965; Hood & Finkelstein, 1986; Hood, 1998). Multiplicative adaptation is complete within 50–100 ms, at least for backgrounds up to about 3 $\log_{10}$ Td (Hayhoe, Benimoff, & Hood, 1987; Hayhoe, Levin, & Koshel, 1992), and subtractive adaptation may follow a comparably rapid time course (Geisler, 1978; Hayhoe et al., 1987), although some evidence suggests that it might be delayed by 200 ms and take as long as 10–15 s to complete (Hayhoe et al., 1992). Neither of these processes, however, is likely to be the direct cause of the delayed S-cone sensitivity loss found in TT2 either because they are too fast or because their recovery is monotonic. It is perhaps worth noting that while multiplicative and subtractive adaptation are convenient descriptors, it is not clear how they are implemented neurally. It seems likely that multiplicative adaptation is predominantly caused by shortening time-constants in the visual pathway. Shortening time constants reduces temporal integration and increases the relative sensitivity to higher temporal frequencies, producing briefer, smaller flash responses (de Lange, 1958a; Kelly, 1961; Roufs, 1972; Stockman, Langendörfer, Smithson, & Sharpe, 2006). Subtractive adaptation, on the other hand, associates light adaptation with high-pass filtering; i.e., relative increases in low-frequency attenuation (e.g., Rider, Henning, & Stockman, 2016). Low-frequency attenuation implies a biphasic flash response (Watson & Nachmias, 1977), but also causes an earlier, lower peak flash response which, in terms of

flash detection, would be indistinguishable from a change in multiplicative gain.

The TT2 phenomenon occurs on 581-nm backgrounds of 4.75 $\log_{10}$ Td or higher. These backgrounds bleach a significant amount of photopigment (more than 74% of the L- and M-cone photopigments in the steady state; see Tables A1 and A2). A reasonable supposition, therefore, is that the suppression is related to the effects of a bleaching photoproduct or intermediary, such as, inactivated forms of metarhodopsin II, metarhodopsin III, or opsin (e.g., Lamb, 1981; Okada, Nakai, & Ikai, 1989; Cornwall & Fain, 1994; Matthews, Cornwall, & Fain, 1996; Leibrock, Reuter, & Lamb, 1998; Zimmermann, Ritter, Bartl, Hofmann, & Heck, 2004). For reviews, see Lamb (2004) or Reuter (2011). Indeed, the rise and fall in S-cone threshold is reminiscent of the production of metarhodopsin III in human rods (see figure 10 of Alpern, 1971)—albeit about 15 times faster.

The idea that intermediate bleaching photoproducts can act like real lights in reducing sensitivity has its roots in the "equivalent background hypothesis," which holds that the after-effects of a bleach are equivalent to a real background light in their effects on visual performance (e.g., Stiles & Crawford, 1932; Crawford, 1937; Geisler, 1979). Given that relatively little is known about the details or timing of *in vivo* human cone photopigment generation in retinoid cycles that involve either the retinal pigment epithelium or Müller cells (Reuter, 2011; Sato & Kefalov, 2016), we will concentrate in this section on defining the dynamics of the lifetime of this hypothetical, but mystery photoproduct (which we call "X").

In our basic model, we suppose that X, which, in the TT2 experiments, is produced by the high intensity background stimulus in the L- and M-cones, acts like a real light at the cone outputs and inhibits S-cone sensitivity at the cone-opponent site in the S-cone pathway (see Figure 1). The delayed inhibition seen early in the data is roughly consistent with the growth and removal of an intermediate bleaching photoproduct, X, in a successive, two-stage chain of first-order
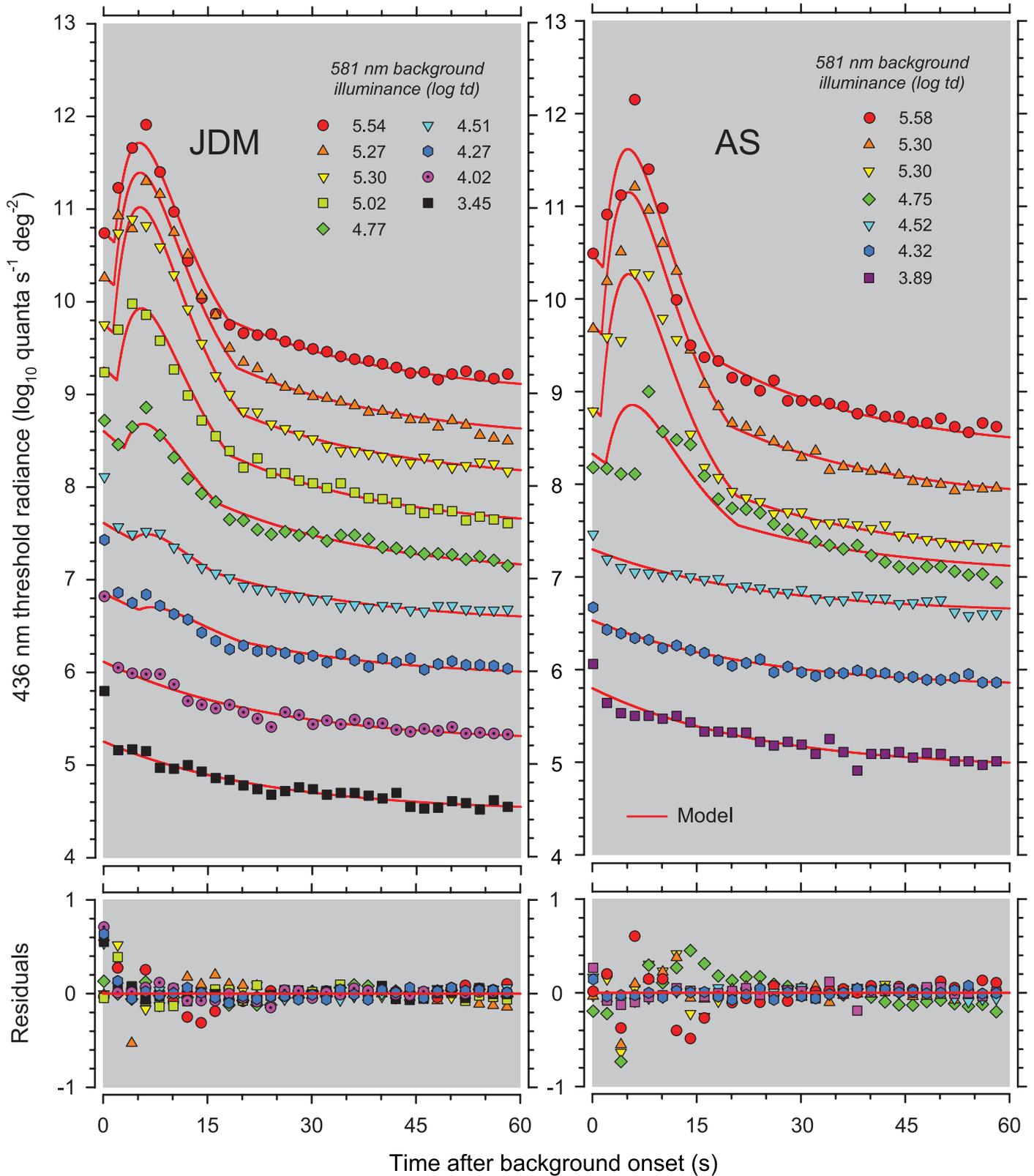
Figure 3. Upper: Threshold radiances for JDM (left panel) and AS (right panel) plotted previously in Figure 2. Details as for Figure 1. The solid red lines are fits of the second model with three common time-constants simultaneously fitted to all the data in both panels. For details, see Table A2 and text. The thresholds 100-ms after the background onset at the four lowest illuminances for JDM and the three lowest illuminances for AS were excluded from the fits. Lower: Residuals.

reactions:

$$A \xrightarrow{\tau_A} X \xrightarrow{\tau_X} C, \quad (1)$$
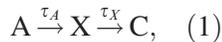
where the initial reactant in the chain, A, decomposes to X with time-constant, τ_A; and X grows according to the depletion of A and decomposes to the final product, C, with a time constant, τ_X. (The time-constant, τ, is the time taken for the decay to reach $1/e$ or 36.8% of its original value or, in the case of growth, to $1 - 1/e$ or 63.2% of its maximum value.)

Equations that give the concentrations of A, X, and C as a function of time are simple to derive and can be found in standard chemistry texts (e.g., House, 2007; Cornish-Bowden, 2012). [A], the concentration of A, changes as a function of time (t, s) according to

$$[A] = [A]_0 e^{-t/\tau_A}, \quad (2)$$

where $[A]_0$ is the initial concentration of A (at $t = 0$), and τ_A is the time-constant, in seconds, of the first reaction. [X], the concentration of X, changes according to

$$[X] = [A]_0 \frac{\tau_X}{\tau_X - \tau_A} \left(e^{-t/\tau_X} - e^{-t/\tau_A} \right), \quad (3)$$

where τ_X is the time-constant of the second reaction.

In terms of applying the model and linking it to the data shown in Figures 2 and 3, a crucial question is how [X] might be related to the threshold intensity, ΔI, required to detect the 436-nm flash against the background and in particular whether the relation between [X] and ΔI is closer to being linear or logarithmic. We discuss the relation between [X] and ΔI further below, but initially we take an empirical approach, based on the form of the data and using Equation (3) for [X], and treat the relation as approximately logarithmic:

$$\log_{10}\Delta I = c_X \frac{\tau_X}{\tau_X - \tau_A} \left(e^{-t/\tau_X} - e^{-t/\tau_A} \right) + v, \quad (4)$$

where ΔI is the measured threshold radiance in quanta s^{-1} deg^{-2}, c_X is the unknown factor that includes both $[A]_0$ from Equation (3) and some gain factor, and v is a vertical logarithmic shift of the function (which corresponds roughly to the ultimate baseline steady-state sensitivity of the S-cone system). We discuss this logarithmic relation below—it has been assumed before in describing dark adaptation data (Dowling, 1960; Rushton, 1961).

In fitting the model of Equation (4) at the four lowest levels for JDM and at the three lowest levels for AS, the model was simplified by removing the first stage A→X and the first time-constant, τ_A, from the fit, thus at the lowest levels:

$$\log_{10}\Delta I = c_X e^{-t/\tau_X} + v. \quad (5)$$

Having just one stage X→C at these levels made the fits much more stable, since, as can be seen in the upper panels of Figure 2, the data at those levels approximate a single exponential decay.

For model fitting, we used the nonlinear regression implemented in SigmaPlot (Systat Software, San Jose, CA) based on the Marquardt-Levenberg algorithm (Levenberg, 1944; Marquardt, 1963). The fit minimizes the sum of the squared differences between the data and the predictions of the model. (Note that for nonlinear regression, R^2 as a measure of goodness-of-fit is problematic—e.g., Kvalseth, 1985; Spiess & Neumeyer, 2010—so that as well as giving R^2 values in Tables A1 and A2, we also give the standard error of the residuals, which can be used to assess the accuracy of the predictions. The residuals are plotted in the lower panels of Figure 2.) The fitted parameters are given below as the parameter ± 1 SE of the fitted parameter.

The solid lines plotted in the upper panels of Figure 2 show the simultaneous fit of Equations (4) or (5) to the data for all background illuminances for JDM (left-hand panel) and AS (right-hand panel). (The fits are, of course, adjusted up or down by the same amount as the data.) In this fit, the same time constants, τ_A and τ_X, were applied across all background illuminances and observers. The best-fitting parameters and their standard errors are given in Table A1 in the Appendix. Given the simplicity of this descriptive model, the fits are remarkably good with an R^2 goodness-of-fit of 0.982, an adjusted R^2 of 0.980, and a SE of the residuals of 0.010 $\log_{10}$ threshold units.

For JDM, the model predictions are generally good, although there are some discrepancies between 10 and 20 s at the 5.54 $\log_{10}$ Td level, between 7 and 15 s at the lower background levels, and between 40 and 60 s at several levels. For AS, the predictions are worse: Discrepancies similar to those for JDM occur between 10 and 20 s in the 5.58 $\log_{10}$ Td data set, but there are other discrepancies between 1 and 20 s in the 4.75 $\log_{10}$ Td level. The model consistently underestimates the data at 100 ms for both observers and overestimates the data after 50 s. Nonetheless, this simple model provides a not unreasonable description of the time course of TT2.

The fit of the Basic model suggests that $\tau_A = 3.09 \pm 0.35$ s and $\tau_X = 7.72 \pm 0.70$ s. It should be noted that the order of time constants and thus the order of the reactions is constrained by our assumption that τ_X alone determines threshold after background onsets of lower illuminances. Without this assumption, the order of τ_A and τ_X is reversible (i.e., we do not know which of A→X or X→C has the shorter time constant).

Discussion

In this section, we discuss some of the implications of the Basic model and consider potential refinements. We recognize that the section is inevitably speculative, because we are attempting to link perceptual data and a perceptually based model to complex processes in cone and postreceptoral neural networks, about which relatively little is known. Nevertheless, we think that some interesting conclusions can be drawn. Lastly, based in part on these conclusions, we present a modified model that provides a slightly better characterization of the data.

Dark and light adaptation, incremental threshold and X

For dark adaptation data, there has been some controversy over the form of the dependence of $\log_{10}\Delta I$ on $1 - p$, the proportion of bleached pigment, where p is the proportion of unbleached pigment. The arguments are relevant here because our models depend on assumptions about the link between $1 - p$, the resulting photoproducts, and ΔI. According to Dowling (1960) and Rushton (1961), during *dark* adaptation the logarithm of threshold, $\log_{10}\Delta I$, is proportional to $1 - p$. More recently, however, Lamb (1981) has suggested that instead the linear threshold, ΔI, is proportional to $1 - p$, except for nearly complete rod bleaches. Similarly, for cones, Pianta and Kalloniatis (2000) have also suggested that in dark adaptation the relation is linear rather than logarithmic. In general, if $1 - p \propto \log_{10}\Delta I$ and the unbleached pigment recovers exponentially (i.e., according to first order kinetics), then a plot of $\log_{10}\Delta I$ against time (i.e., the same log-linear axes as in Figures 2 and 3), should follow an exponential decay, whereas if $1 - p \propto \Delta I$ the decay of $\log_{10}\Delta I$ should follow a straight line. Over their *whole* range, dark adaptation curves plotted on log-linear plots are clearly better described by an exponential decay rather than by a straight line (e.g., Pugh, 1976). Yet, by assuming that dark adaptation measurements reflect successive exponential recoveries of several photoproducts, each of which elevates threshold *linearly*, the recovery curves can be fitted by overlapping line segments (e.g., Lamb, 1981; Pianta & Kalloniatis, 2000). In practice, however, there is often little difference between fits of exponentials and fits of overlapping line segments to recovery data either for rod (see figures in Lamb, 1981) or for cone (see figures in Pianta & Kalloniatis, 2000) vision. We could similarly fit monotonically falling pieces of the data in Figures 2 and 3 with overlapping line segments, but

without some theoretical underpinnings such fits would be largely meaningless.

Of course, the data shown in Figures 2 and 3 are *light* adaptation rather than *dark* adaptation measurements, and some are made at levels that cause significant photopigment bleaching (see Tables A1 and A2). Thus, the question of whether ΔI is proportional to [X] or not may be moot, since nonlinearities introduced by the processes of light adaptation (e.g., Stockman et al., 2006) will affect thresholds in addition to any putative effects of [X]. As introduced above, such processes could include multiplicative adaptation, subtractive adaptation, and response compression. Multiplicative adaptation, for example, is complete within 50–100 ms (Hayhoe et al., 1987; Hayhoe et al., 1992), and thus is much faster than the time constants associated with X. Consequently, if X alters sensitivity *prior* to the multiplicative stage, its effects will be partially compensated for by multiplicative adaptation. Our model suggests that *if* [X] is indeed proportional to ΔI, then these nonlinear adaptational processes can be approximated by a logarithmic transform. Thus, plotted on log-linear coordinates as in Figures 2 and 3, light adaptation follows the negative-exponential rise and exponential fall shown by the fitted curves in Figure 2. (It should be noted that the data in Figures 2 and 3 are inconsistent with linear versions of the same model in which thresholds rise rapidly but with a decelerating slope and then fall linearly.)

Alternatively, the effect of [X] could occur *after* multiplicative and perhaps subtractive processes of light adaptation. The logarithmic relation between [X] and ΔI might then reflect a subsequent logarithmic compression. In terms of the sequential light adaptation model of Hayhoe, Benimoff, and Hood (1987) in which the order of adaptation processes is multiplicative, subtractive, and compressive, the effect of [X] would apply after the multiplicative and subtractive stages but before the compressive (saturating) nonlinearity. We favor the proposal that [X] acts after the multiplicative process (and perhaps after the subtractive process), since that order explains why the effect of [X] is not attenuated by multiplicative and subtractive stages.

Since we are measuring the indirect effect on the S-cones of [X] produced in the L- and M-cones, the logarithmic compression is likely to be related to the sigmoidal compressive nonlinearity at the cone-opponent second site where the L- and M-cone and S-cone signals interact (see Figure 1).

We next consider how [X] might be related to ongoing photoisomerizations produced by the yellow-appearing backgrounds.

Dynamics of [X] and photopigment depletion

In preliminary versions of the Basic model, we allowed τ_A and τ_X to vary across background illuminances and observers. This difference led to relatively unstable solutions with large standard errors, yet neither τ_A nor τ_X varied systematically with background illuminance at the higher levels that produce the TT2 phenomenon. Indeed, we found that we could simplify the model by fixing τ_A and τ_X across background illuminances and observers, and still obtain a good fit that only reduced the R^2 goodness-of-fit from 0.996 to 0.982 and doubled the *SE* of the residuals from 0.005 to 0.010 $\log_{10}$ threshold units. We infer therefore that the time constants τ_A and τ_X are approximately independent of background illuminance. But, given that τ_A and τ_X are independent of background illuminance, how might [X] relate to the rate of photopigment bleaching and the initial production of the active metarhodopsin II that initiates the transduction cascade?

The rate of photoisomerizations and thus the rate of photopigment bleaching that occurs after the background onset are proportional to the intensity of the light and the amount of unbleached pigment. The amount of pigment changes over time as the opposing forces of regeneration and bleaching approach a steady state. Thus, according to Rushton and Henry (1968):

$$\frac{dp}{dt} = \frac{(1-p)}{120} - \frac{Ip}{120\,I_0}, \quad (6)$$

where p is the proportion of unbleached pigment, I is the background illuminance, and I_0 is a constant that is equal to the background illuminance at which 50% of the pigment is bleached in the final steady state. Given that $p \approx 1$ at background onset, the rate of change of p at early times is approximately $dp/dt \approx -I/120\,I_0$. Thus, the number of photoisomerizations per unit time is proportional to the background illuminance, I, for small t. The solution of Equation 6 for p is:

$$p(t) = \frac{I_0}{I+I_0} + \frac{I}{I+I_0} e^{-\frac{I+I_0}{120\,I_0}t}, \quad (7)$$

which is an exponential decay with a time constant of $120\,I_0/(I+I_0)$. If TT2 is due to the effects of the real light on the L- and M-cones, then we would expect the corresponding time constant(s) to change dramatically with light level. The shortening of these time-constants with increasing background illuminances, can be seen clearly in suction electrode recordings from primate cone photoreceptors in figure 12 of Schnapf, Nunn, Meister, & Baylor (1990), although in the course in such experiments the outer segment is necessarily separated from the pigment epithelium.

Assuming an I_0 of 4.30 $\log_{10}$ Td, the time constants for JDM for background illuminances between 4.77 and 5.54 $\log_{10}$ Td that show a clear TT2 effect should change from 30.4 to 6.53 s, and the time constants for AS for background illuminances between 4.75 and 5.58 $\log_{10}$ Td that similarly show a clear TT2 effect they should change from 31.4s to 5.98 s. By contrast, the time constants for the lifetime of X are roughly constant across these illuminances at 3.09 and 7.73 s, which correspond to the time constants at the highest illuminances.

These comparisons suggest that X is unlikely to be a bleaching photoproduct in the direct cone retinoid cycle represented by Equation (7), since it is independent of the rate of photoisomerization produced by the backgrounds. Consequently, it may represent a subsidiary or parallel reaction path that becomes significant when the rate of bleaching is high. We speculate that the reaction that produces [X] may be important as a reactant buffer.

Modified model and fit

We tried several modifications to our basic model in an attempt not only too improve the fits, but also to try to understand more about the underlying mechanisms. Most modifications, however, produced relatively small improvements that were offset by increases in the standard errors of the fitted parameters. One plausible modification, described next, is related to idea that the effect of [X] on threshold is applied after the direct effect of the real light, which is subject to the processes of multiplicative and subtractive adaption and is therefore to some extent independent of those processes. By contrast, the effect of real light, produced by photoisomerizations, will be subject to the usual processes of light adaptation (see above and Figure 1).

As before, we assume that [X] is proportional to $\log_{10}\Delta I$. We additionally assume that it only reduces sensitivity if it exceeds the effect of other processes of light adaptation, which could be first-site or second-site processes. We find that these other unknown, slow processes can be summarized by another exponential decay with a fixed time constant, which we refer to as τ_S. The model is described by:

$$\log_{10}\Delta I = \max\left[c_X \frac{\tau_X}{\tau_A - \tau_X}\left(e^{-t/\tau_A} - e^{-t/\tau_X}\right), c_S e^{-t/\tau_S}\right] + v, \quad (8)$$

where c_S scales the slow exponential decay and the "max" function returns the greater of $c_X \frac{\tau_X}{\tau_A - \tau_X}\left(e^{-t/\tau_A} - e^{-t/\tau_X}\right)$ and $c_S e^{-t/\tau_S}$.

We adopted the approach of taking the greater of $c_X \frac{\tau_X}{\tau_A - \tau_X}\left(e^{-t/\tau_A} - e^{-t/\tau_X}\right)$ and $c_S e^{-t/\tau_S}$ based mainly on the form of the data, but also on the assumption that for [X] to have a measureable effect it must exceed a threshold determined by other adaptation processes. It

is particularly interesting to note that the slow exponential decay can also account for the data at the first few time-points at and above 4.27 $\log_{10}$ photopic Td for JDM and at and above 4.75 $\log_{10}$ photopic Td for AS.

The red continuous lines in Figure 3 show a simultaneous fit of Equation (8) to all the data for JDM and AS. In this version of the model, we fixed τ_A, τ_X, and τ_S across background illuminances and observers, and allowed only c_X, c_S, and v to vary. As for the first model, this model was simplified to a single exponential recovery at lower background levels to avoid instability in the fits. This was achieved by setting c_X in Equation (8) to 0, and was necessary only at the two lowest levels for JDM and at the three lowest for AS. The best-fitting parameters and their standard errors are given in Table A2 in the Appendix. The fit of the model suggests that $\tau_A = 4.15 \pm 0.62$ s and $\tau_X = 6.79 \pm 1.00$ s and that $\tau_S = 23.94 \pm 1.42$ s to account for slow overall recovery. Note that the order of τ_A and τ_X is reversible (i.e., we do not know which of A→X or X→C is faster).

The final model fits have an R^2 goodness-of-fit of 0.995, an adjusted R^2 of 0.995, and a standard error of the estimate of the residuals of 0.005 $\log_{10}$ threshold units. The lower panels of Figure 3 show the residuals. The model predictions for JDM are particularly good and characterize the delayed sensitivity loss for backgrounds from 4.27 to 5.54 $\log_{10}$ photopic Td level remarkably well. The predictions for AS are also good, except for the 4.75 $\log_{10}$ photopic Td level (green diamonds), where there are substantial deviations at shorter times. According to the fits, the peak sensitivity loss occurs at 5.2 s for both observers. (Note that we excluded the 100-ms points from the modified fit at the four lowest luminances for JDM and the three lowest for AS. These points distorted the fits, and we suspect that at low illuminances the immediate loss of sensitivity is due mainly to effects of masking operating over a window of approximately 100 ms rather than to the effects of bleaching or adaptation; see, for example, Bachmann & Francis, 2014.)

The slow recovery represented by $\tau_S = 23.94 \pm 1.42$ s could reflect subtractive adaptation, which Hayhoe, Levin, and Koshel (1992) have reported to take up to 10–15 s to compete, but is more likely to reflect the hypothetical restoring force of the cone-opponent site postulated by Pugh and Mollon (1979) to explain the exponential recovery of S-cone sensitivity found in TT1 after the offset of yellow backgrounds of less than about 5 $\log_{10}$ Td (see above). In fact, our estimate of τ_S of 23.94 s falls nicely between the estimates of the time constant for two observers by Augenstein and Pugh (1977) of 15.45 and 27.57 s.

One final class of model is illustrated for completeness in the lower panel of Figure 1. The orange arrow from the L- and M-cone to the S-cones represents a suppressive interaction that might arise because of a substance produced by the bleach that permeates between the cones, or because of some competition for limited resources (Trevor Lamb, personal communication).

Possible identity of X

To identify X, all we have to do, in principle, is to find a successive pair of reactions indirectly associated with one of the two cone photopigment recovery cycles with time-constants of about 3.6 s and 7.3 s in either order. In practice, however, such an identification is not straightforward, mainly because relatively little is known about the cone recovery cycles. Most relevant *in vivo* data are from rods, in which reactions are generally slower than in cones, and only relate to the rod retinoid cycle that involves the pigment epithelium (Lamb & Pugh, 2004). The available photochemical data from cones are often obtained at low temperatures and in detergent solutions, and so underestimate the reaction time-constants likely to apply in photoreceptors at body temperature (reviewed in Golobokova & Govardovskii, 2006). Importantly, photopigment regeneration in cones is complicated because, in addition to the retinoid cycle that involves the retinal pigment epithelium used also by rods, cones have an alternative retina cycle that involves Müller cells (e.g., Mata, Radu, Clemmons, & Travis, 2002; Wang & Kefalov, 2009; Kolesnikov, Tang, Parker, Crouch, & Kefalov, 2011; Wang & Kefalov, 2011).

Acknowledgments

Commercial relationships: none.
Corresponding author: Andrew Stockman.
Email: a.stockman@ucl.ac.uk.
Address: UCL Institute of Ophthalmology, University College London, London, UK.

References

Alpern, M. (1971). Rhodopsin kinetics in the human eye. *Journal of Physiology*, *217*(2), 447–471.

Augenstein, E. J., & Pugh, E. N., Jr. (1977). The dynamics of the π_1 color mechanism: Further evidence for two sites of adaptation. *Journal of Physiology*, *272*, 247–281.

Bachmann, T., & Francis, G. (2014). *Visual masking: Studying perception, attention, and consciousness.* San Diego, CA: Academic Press.

Baker, H. D. (1949). The course of foveal light adaptation measured by the threshold intensity increment. *Journal of the Optical Society of America*, *39*(2), 172–179.

Barlow, H. B. (1965). Optic nerve impulses and Weber's Law. *Cold Spring Harbor Symposia on Quantitative Biology*, *30*, 539–546.

Boynton, R. M. (1979). *Human color vision*. New York, NY: Holt, Rinehart and Winston.

Cornish-Bowden, A. (2012). *Fundamentals of enzyme kinetics* (4th ed.). Weinheim, Germany: Wiley-VCH.

Cornsweet, T. N., & Teller, D. Y. (1965). Relation of increment thresholds to brightness and luminance. *Journal of the Optical Society of America*, *55*(10), 1303–1308.

Cornwall, M. C., & Fain, G. L. (1994). Bleached pigment activates transduction in isolated rods of the salamander retina. *Journal of Physiology*, *480*, 261–279.

Crawford, B. H. (1937). The change of visual sensitivity with time. *Proceedings of the Royal Society of London. Series B*, *123*(830), 69–89.

de Lange, H. (1958a). Research into the dynamic nature of the human fovea-cortex systems with intermittent and modulated light. I. Attenuation characteristics with white and colored light. *Journal of the Optical Society of America*, *48*, 777–784.

de Lange, H. (1958b). Research into the dynamic nature of the human fovea-cortex systems with intermittent and modulated light. II. Phase shift in brightness and delay in color perception. *Journal of the Optical Society of America*, *48*, 784–789.

Dowling, J. E. (1960). Chemistry of visual adaptation in the rat. *Nature*, *188*, 114–118.

Eisner, A., & MacLeod, D. I. A. (1980). Blue sensitive cones do not contribute to luminance. *Journal of the Optical Society of America*, *70*, 121–123.

Geisler, W. S. (1978). Adaptation, afterimage and cone saturation. *Vision Research*, *18*, 279–289.

Geisler, W. S. (1979). Evidence for the equivalent-background hypothesis in cones. *Vision Research*, *19*(7), 799–805.

Golobokova, E. Y., & Govardovskii, V. I. (2006). Late stages of visual pigment photolysis in situ: Cones vs. rods. *Vision Research*, *46*(14), 2287–2297.

Guth, S. L., Alexander, J. V., Chumbly, J. I., Gillman, C. B., & Patterson, M. M. (1968). Factors affecting luminance additivity at threshold among normal and color-blind subjects and elaborations of a trichromatic-opponent color theory. *Vision Research*, *8*(7), 913–928.

Hayhoe, M. M., Benimoff, N. I., & Hood, D. C. (1987). The time course of multiplicative and subtractive adaptation processes. *Vision Research*, *27*, 1981–1996.

Hayhoe, M. M., Levin, M. E., & Koshel, R. J. (1992). Subtractive processes in light adaptation. *Vision Research*, *32*(2), 323–333.

Hood, D. C. (1998). Lower-level visual processing and models of light adaptation. *Annual Review of Psychology*, *49*, 503–535.

Hood, D. C., & Finkelstein, M. A. (1986). Sensitivity to light. In K. Boff, L. Kaufman, & J. Thomas (Eds.), *Handbook of perception and human performance (Vol. 1*, pp. 5-1-5-66). New York, NY: Wiley.

House, J. E. (2007). *Principles of chemical kinetics* (2nd ed.). Burlington, MA: Academic Press.

Kelly, D. H. (1961). Visual responses to time-dependent stimuli I. Amplitude sensitivity measurements. *Journal of the Optical Society of America*, *51*, 422–429.

Kolesnikov, A. V., Tang, P. H., Parker, R. O., Crouch, R. K., & Kefalov, V. J. (2011). The mammalian cone visual cycle promotes rapid M/L-cone pigment regeneration independently of the interphotoreceptor retinoid-binding protein. *Journal of Neuroscience*, *31*(21), 7900–7909.

Kvalseth, T. O. (1985). Cautionary note about R^2. *The American Statistician*, *39*(4), 279–285.

Lamb, T. D. (1981). The involvement of rod photoreceptors in dark adaptation. *Vision Research*, *21*(12), 1773–1782.

Lamb, T. D., & Pugh, E. N., Jr. (2004). Dark adaptation and the retinoid cycle of vision. *Progress in Retinal and Eye Research*, *23*(3), 307–380.

Lee, J., & Stromeyer, C. F., III. (1989). Contribution of human short-wave cones to luminance and motion detection. *Journal of Physiology*, *413*, 563–593.

Leibrock, C. S., & Lamb, T. D. (1997). Effect of hydroxylamine on photon-like events during dark

adaptation in toad rod photoreceptors. *Journal of Physiology*, *501*, 97–109.

Leibrock, C. S., Reuter, T., & Lamb, T. D. (1998). Molecular basis of dark adaptation in rod photoreceptors. *Eye*, *12*, 511–520.

Levenberg, K. (1944). A method for the solution of certain non-linear problems in least squares. *Quarterly of Applied Mathematics*, *2*(2), 164–168.

Luther, R. (1927). Aus dem Gebiet der Farbreizmetrik [On color stimulus metrics]. *Zeitschrift für technische Physik*, *8*, 540–558.

Marquardt, D. W. (1963). An algorithm for least-squares estimation of nonlinear parameters. *Journal of the Society for Industrial and Applied Mathematics*, *11*(2), 431–441.

Mata, N. L., Radu, R. A., Clemmons, R. C., & Travis, G. H. (2002). Isomerization and oxidation of vitamin a in cone-dominant retinas: A novel pathway for visual-pigment regeneration in daylight. *Neuron*, *36*(1), 69–80.

Matthews, H. R., Cornwall, M. C., & Fain, G. L. (1996). Persistent activation of transducin by bleached rhodopsin in salamander rods. *Journal of General Physiology*, *108*, 557–563.

Mollon, J. D. (1982a). Color vision. *Annual Review of Psychology*, *33*, 41–85.

Mollon, J. D. (1982b). *A taxonomy of tritanopias*. Paper presented at the Colour Vision Deficiencies VI. Proceedings of the International Symposium. Berlin, Germany and The Hague, the Netherlands.

Mollon, J. D., & Polden, P. G. (1975). Colour illusion and evidence for interaction between cone mechanisms. *Nature*, *258*(5534), 421–422.

Mollon, J. D., & Polden, P. G. (1976). Absence of transient tritanopia after adaptation to very intense yellow light. *Nature*, *259*(5544), 570–572.

Mollon, J. D., & Polden, P. G. (1977). An anomaly in the response of the eye to light of short wavelengths. *Philosophical Transactions of the Royal Society of London. Series B*, *278*(960), 207–240.

Mollon, J. D., Stockman, A., & Polden, P. G. (1987). Transient tritanopia of a second kind. *Vision Research*, *27*(4), 637–650.

Okada, D., Nakai, T., & Ikai, A. (1989). Transducin activation by molecular species of rhodopsin other than meta rhodopsin II. *Photochemistry and Photobiology*, *49*(2), 197–203.

Pianta, M. J., & Kalloniatis, M. (2000). Characterisation of dark adaptation in human cone pathways: An application of the equivalent background hypothesis. *Journal of Physiology*, *528*(Pt 3), 591–608.

Polden, P. G., & Mollon, J. D. (1980). Reversed effect of adapting stimuli on visual sensitivity. *Proceedings of the Royal Society of London. Series B*, *210*(1179), 235–272.

Pugh, E. N., Jr. (1976). Rushton's Paradox: Rod dark adaptation after flash photolysis. *Journal of Physiology*, *248*, 413–431.

Pugh, E. N., Jr., & Mollon, J. D. (1979). A theory of the π_1 and π_3 color mechanisms of Stiles. *Vision Research*, *20*, 293–312.

Reuter, T. (2011). Fifty years of dark adaptation 1961–2011. *Vision Research*, *51*(21), 2243–2262.

Rider, A. T., Henning, G. B., & Stockman, A. (2016). Light adaptation and the human temporal response revisited. *Journal of Vision*, *16*(12): 387, https://doi.org/10.1167/16.12.387. [Abstract]

Ripamonti, C., Woo, W. L., Crowther, E., & Stockman, A. (2009). The S-cone contribution to luminance depends on the M- and L-cone adaptation levels: Silent surrounds? *Journal of Vision*, *9*(3): 10, 1–16, https://doi.org/10.1167/9.3.10. [PubMed] [Article]

Roufs, J. A. J. (1972). Dynamic properties of vision-I. Experimental relationships between flicker and flash thresholds. *Vision Research*, *12*, 261–278.

Rushton, W. A. H. (1961). Dark adaptation and the regeneration of rhodopsin. *Journal of Physiology*, *156*, 166–178.

Rushton, W. A. H., & Henry, G. H. (1968). Bleaching and regeneration of cone pigments in man. *Vision Research*, *8*(6), 617–631.

Sato, S., & Kefalov, V. J. (2016). cis Retinol oxidation regulates photoreceptor access to the retina visual cycle and cone pigment regeneration. *Journal of Physiology*, *594*(22), 6753–6765.

Schnapf, J. L., Nunn, B. J., Meister, M., & Baylor, D. A. (1990). Visual transduction in cones of the monkey Macaca fascicularis. *Journal of Physiology*, *427*, 681–713.

Schrödinger, E. (1925). Über das Verhältnis der Vierfarben zur Dreifarbentheorie [On the relationship of four-color theory to three-color theory]. *Sitzungberichte. Abt. 2a, Mathematik, Astronomie, Physik, Meteorologie und Mechanik. Akademie der Wissenschaften in Wien, Mathematisch-Naturwissenschaftliche Klasse*, *134*, 471–490.

Smith, V. C., & Pokorny, J. (1975). Spectral sensitivity of the foveal cone photopigments between 400 and 500 nm. *Vision Research*, *15*, 161–171.

Spiess, A.-N., & Neumeyer, N. (2010). An evaluation of R^2 as an inadequate measure for nonlinear models in pharmacological and biochemical re-

search: A Monte Carlo approach. *BMC Pharmacology*, *10*(6), 1–11.

Stiles, W. S. (1949). Incremental thresholds and the mechanisms of colour vision. *Documenta Ophthalmologica*, *3*, 138–163.

Stiles, W. S. (1978). *Mechanisms of colour vision*. London, UK: Academic Press.

Stiles, W. S., & Crawford, B. H. (1932). Equivalent adaptation levels in localised retinal areas. In A. O. Rankine & A. Ferguson (Chairmen), report of a joint discussion on vision held on June 3, 1932, at the Imperial College of Science by the Physical and Optical Societies (pp. 194–211). Cambridge: Cambridge University Press.

Stockman, A., & Brainard, D. H. (2010). Color vision mechanisms. In M. Bass, C. DeCusatis, J. Enoch, V. Lakshminarayanan, G. Li, C. Macdonald, V. Mahajan, & E. van Stryland (Eds.), *The Optical Society of America handbook of optics* (3rd ed., *Vol. III*: *Vision and vision optics*, pp. 11.11–11.104). New York, NY: McGraw Hill.

Stockman, A., Langendörfer, M., Smithson, H. E., & Sharpe, L. T. (2006). Human cone light adaptation: From behavioral measurements to molecular mechanisms. *Journal of Vision*, *6*(11):5, 1194–1213, https://doi.org/10.1167/6.11.5. [PubMed] [Article]

Stockman, A., MacLeod, D. I. A., & DePriest, D. D. (1991). The temporal properties of the human short-wave photoreceptors and their associated pathways. *Vision Research*, *31*(2), 189–208.

Stockman, A., & Sharpe, L. T. (2000). Spectral sensitivities of the middle- and long-wavelength sensitive cones derived from measurements in observers of known genotype. *Vision Research*, *40*(13), 1711–1737.

Stockman, A., Sharpe, L. T., & Fach, C. C. (1999). The spectral sensitivity of the human short-wavelength cones. *Vision Research*, *39*(17), 2901–2927.

Walls, G. L. (1955). A branched-pathway schema for the color-vision system and some of the evidence for it. *American Journal of Ophthalmology*, *39*(2), 8–23.

Wang, J.-S., & Kefalov, V. J. (2009). An alternative pathway mediates the mouse and human cone visual cycle. *Current Biology*, *19*(19), 1665–1669.

Wang, J.-S., & Kefalov, V. J. (2011). The cone-specific visual cycle. *Progress in Retinal and Eye Research*, *30*(2), 115–128.

Watson, A. B., & Nachmias, J. (1977). Patterns of temporal interaction in the detection of gratings. *Vision Research*, *17*(8), 893–902.

Zimmermann, K., Ritter, E., Bartl, F. J., Hofmann, K. P., & Heck, M. (2004). Interaction with Transducin depletes Metarhodopsin III: A regulated retinal storage in visual signal transduction? *Journal of Biological Chemistry*, *279*(46), 48112–48119.

Appendix

Background	Log td	3.45	4.02	4.27	4.51	4.77	5.02	5.30	5.27	5.54
	% bleach	12.4	34.4	48.3	61.9	74.7	84.0	90.9	90.3	94.6
JDM	τ_A	Single stage only				3.09 ±0.35				
	τ_X	7.73±0.70								
	c_X	0.89 ±0.23	1.05 ±0.23	1.23 ±0.23	1.43 ±0.24	6.31 ±1.39	9.75 ±2.01	12.43 ±2.51	11.91 ±2.42	11.04 ±1.06
	v	6.66 ±0.05	6.93 ±0.05	7.14 ±0.05	7.26 ±0.05	7.37 ±0.05	7.35 ±0.06	7.33 ±0.06	7.31 ±0.06	7.29 ±0.06

Background	Log td	3.89	4.32	4.52	4.75	5.30	5.30	5.58
	% bleach	28.0	51.2	62.4	73.8	90.9	90.9	95.0
AS	τ_A	Single stage only			3.09 ±0.35			
	τ_X	7.73±0.70						
	c_X	0.89 ±0.18	0.75 ±0.18	0.69 ±0.18	7.38 ±1.62	12.89 ±2.60	13.90 ±2.79	13.12 ±2.64
	v	6.63 ±0.05	6.97 ±0.05	7.27 ±0.05	7.28 ±0.05	6.97 ±0.06	7.13 ±0.06	7.22 ±0.06

Table A1. Best-fitting model parameters for the two time-constant Basic model for JDM (upper panel) and AS (lower panel). *Notes*: The % bleach values were calculated using the standard equation on the assumption that the half-bleach constant $I_0 = 10^{4.3}$ Td (Rushton & Henry, 1968): $p = \frac{I}{I+I_0}$, where p is the fraction of bleached pigment and I is the background illuminance in trolands. For other details, see text.

Background	Log td	3.45	4.02	4.27	4.51	4.77	5.02	5.30	5.27	5.54
	% bleach	12.4	34.4	48.3	61.9	74.7	84.0	90.9	90.3	94.6
JDM	τ_A	Single stage only		4.15±0.62						
	τ_X			6.79±1.00						
	τ_S	23.94±1.42								
	c_X	0		3.11 ±1.85	3.71 ±2.19	6.09 ±3.58	8.73 ±5.16	10.62 ±6.28	10.38 ±6.13	9.73 ±5.74
	c_S	0.76 ±0.09	0.87 ±0.09	0.84 ±0.13	1.05 ±0.13	1.55 ±0.11	1.78 ±0.13	1.72 ±0.13	1.80 ±0.13	1.82 ±0.13
	v	6.49 ±0.04	6.74 ±0.04	6.95 ±0.05	7.03 ±0.05	7.04 ±0.05	7.01 ±0.05	7.04 ±0.05	6.98 ±0.05	6.96 ±0.06

Background	Log td	3.89	4.32	4.52	4.75	5.30	5.30	5.58
	% bleach	28.0	51.2	62.4	73.8	90.9	90.9	95.0
AS	τ_A	Single stage only			4.15±0.62			
	τ_X				6.79±1.00			
	τ_S	23.94±1.42						
	c_X	0			6.66 ±3.94	10.97 ±6.49	11.99 ±7.09	11.62 ±6.86
	c_S	0.87 ±0.08	0.73 ±0.08	0.69 ±0.08	1.36 ±0.13	1.63 ±0.14	1.94 ±0.13	2.16 ±0.13
	v	6.42 ±0.04	6.80 ±0.04	7.10 ±0.04	7.02 ±0.05	6.69 ±0.05	6.79 ±0.06	6.82 ±0.06

Table A2. Best-fitting parameters for the three time-constant modified model for JDM (upper panel) and AS (lower panel). *Notes*: For other details, see Table A1 and text.